ORIGINAL ARTICLE

Delineation of shallow resistivity structure in the city of Burdur, SW Turkey by vertical electrical sounding measurements

Çağlayan Balkaya · M. Ali Kaya · Gökhan Göktürkler

Abstract The city of Burdur, which is built on an alluvium aquifer, is located in one of the most seismically active zones in southwestern Turkey. The soil properties in the study site are characterized by unconsolidated and water-saturated sediments including silty, clayey and sandy units, and shallow groundwater level is the other characteristic of the site. Thus, the city is under soil liquefaction risk during a large earthquake. A resistivity survey including 189 vertical electrical sounding (VES) measurements was carried out in 2000 as part of a multidisciplinary project aiming to investigate settlement properties in Burdur city and its vicinity. In the present study, the VES data acquired by using a Schlumberger array were re-processed with 1D and 2D inversion techniques to determine liquefaction potential in the study site. The results of some 1D interpretations were compared to the data from several wells drilled during the project. Also, the groundwater level map that was previously obtained by hydrological studies was extended toward north by using the resistivity data. 2D least-squares inversions were performed along nine VES profiles. This provided very useful information on vertical and horizontal extends of geologic units and water content in the subsurface. The study area is characterized by low resistivity distribution ($<150 \ \Omega$m) originating from high fluid content in the subsurface. Lower resistivity ($3–30 \ \Omega$m) is associated with the Quaternary and the Tertiary lacustrine sediments while relatively high resistivity ($40–150 \ \Omega$m) is related to the Quaternary alluvial cone deposits. This study has also shown that the resistivity measurements are useful in the estimation of liquefaction risk in a site by providing information on the groundwater level and the fluid content in the subsurface. Based on this, we obtained a liquefaction hazard map for the study area. The liquefaction potential was classified by considering the resistivity distributions from 2D inversion of the VES profiles, the types of the sediments and the extended groundwater level map. According to this map, the study area was characterized by high liquefaction hazard risk.

Keywords Vertical electrical sounding · Resistivity · Inversion · Liquefaction · Burdur · Turkey

Introduction

Earthquakes are one of the most destructive natural hazards which can cause some secondary events including tsunami, soil liquefaction and landslide (US National Research Council 2003). Among them, damages related to the liquefaction have been considered seriously since the 1964 Niigata, Japan earthquake (Kanıbir et al. 2006). The soil liquefaction typically occurs in the localities which are composed of loose, water-saturated sands and silts (Youd 1993). It is commonly observed in coastal areas and along river beds, where alluvial or deltaic deposits are present (Bird and Bommer 2004). During an earthquake, shaking increases pore water pressure and results in decreased effective stress yielding reduced shear strength in the material. Thus, material behaves like a viscous liquid which causes buildings to sink into the ground or tilt

Ç. Balkaya (✉) · G. Göktürkler
Engineering Faculty, Department of Geophysics,
Dokuz Eylul University, Tınaztepe Campus,
35160 Buca/Izmir, Turkey
e-mail: caglayan.balkaya@deu.edu.tr

M. A. Kaya
Department of Geophysics, Çanakkale Onsekiz Mart University,
17020 Canakkale, Turkey

(Youd 1993). Table 1 shows some of the earthquakes generated major liquefaction-induced damages in various countries in the world.

The study area is located in the city of Burdur, a provincial capital in southwestern Turkey (Fig. 1a). Considering soil liquefaction potential during a large earthquake, the city has some disadvantages. First of all, it is located along the coastal area of the Burdur Lake, which is a large saline lake, and thus it sits on alluvial deposits (Fig. 1b). Second of all, the depth to the groundwater level is very shallow in the area. This is one of the most important factors increasing damages in the liquefaction together with earthquake magnitude, basin structure, peak ground velocity and liquefaction susceptibility of soils (Terzaghi et al. 1996). According to Davraz et al. (2003), the depth to the groundwater level was about 10 m within the Burdur city, and there are a number of streams flowing across the city throughout the Burdur Lake. Their study also revealed that lacustrine sand levels together with shallow groundwater level had potential for liquefaction. Third of all, there is a fault zone, called as the Burdur fault, across the city, which is able to generate destructive earthquakes (Fig. 1b). Thus, the city is under a serious soil liquefaction risk as it had experienced during the earthquake occurred in 1971. Davraz et al. (2003) reports that the geological evidences of this earthquake-induced liquefaction are still observed in the field.

A multi-disciplinary project has been performed by collaboration of geology, geophysics and civil engineering departments of the Suleyman Demirel University, Isparta, Turkey in 2000. The project aimed to investigate the metropolitan area of the city and its surroundings for settlement properties. As a part of this project, a geoelectrical survey including resistivity and self-potential (SP) methods

was carried out in the study area (Balkaya 2002). The SP study and its results are out of the scope of the present paper; hence they are not discussed here. The resistivity is the most used geoelectrical method in near-surface geophysical studies. According to the problem which will be investigated, data acquisition is usually divided into three categories. These are electrical profiling (EP), vertical electrical sounding (VES) and electrical resistivity imaging (ERI). The EP method is sensitive to lateral resistivity changes at a fixed depth of investigation. The VES method measures resistivity changes with respect to the depth. The last method, the ERI, yields information on resistivity change in both vertical and lateral directions because it collects data with a technique, which is a combination of VES and EP. The VES method has been successfully used by a number of researchers in various fields of application including groundwater investigations (Devi et al. 2001; Gowd 2004; Lenkey et al. 2005; Hamzah et al. 2007), groundwater contamination studies (Frohlich et al. 1994, Karlık and Kaya 2001; Kundu et al. 2002; Park et al. 2007), saltwater intrusion problems (Edet and Okereke 2001; Hodlur et al. 2006; Song et al. 2007), geothermal explorations (El-Qady et al. 2000; Majumdar et al. 2000), and rarely in archaeological prospection (El-Qady et al. 1999; Ibrahim et al. 2002). Moreover, the resistivity method is used in liquefaction studies. Beroya and Aydin (2007) performed some VES measurements to define subsurface geometry and some features of the geomorphological model for their study area. Wolf et al. (1998, 2006) used some resistivity profiling surveys in an earthquake-induced liquefaction site to investigate several features such as sand dikes and sand blows in near-surface strata.

In the present study, the VES data were interpreted by using both one-dimensional (1D) and two-dimensional

Table 1 The earthquakes caused the soil liquefaction and damage (after Bird and Bommer 2004)

Name	Year	Country	Magnitude (M_w)	Damage		
				Buildings	Transportation	Utilities
Loma Prieta	1989	USA	6.9	•	•	•
Manjil	1990	Iran	7.7	★	Δ	•
Luzon	1990	Philippines	7.1	★	★	★
Limon	1991	Costa Rica	7.4	Δ	★	★
Erzincan	1992	Turkey	6.7	•	•	Δ
Manzanillo	1995	Mexico	7.6	★	★	Δ
Kobe	1995	Japan	6.9	•	★	•
Adana-Ceyhan	1998	Turkey	5.2	•	•	•
Kocaeli	1999	Turkey	7.4	★	•	★
Chi Chi	1999	Taiwan	7.6	★	•	★
Düzce	1999	Turkey	7.2	Δ	Δ	Δ
El Salvador	2001	El Salvador	7.6	•	★	Δ

Δ: hazard not reported, or reported but no mention of damage; •: minor or moderate damage; ★: major damage

Fig. 1 a Location map; **b** the study area together with the faults (after Ertunç et al. 2001). **c** Location of the Vertical Electrical Sounding (VES) points, wells and the sounding profiles used in 2D inversion
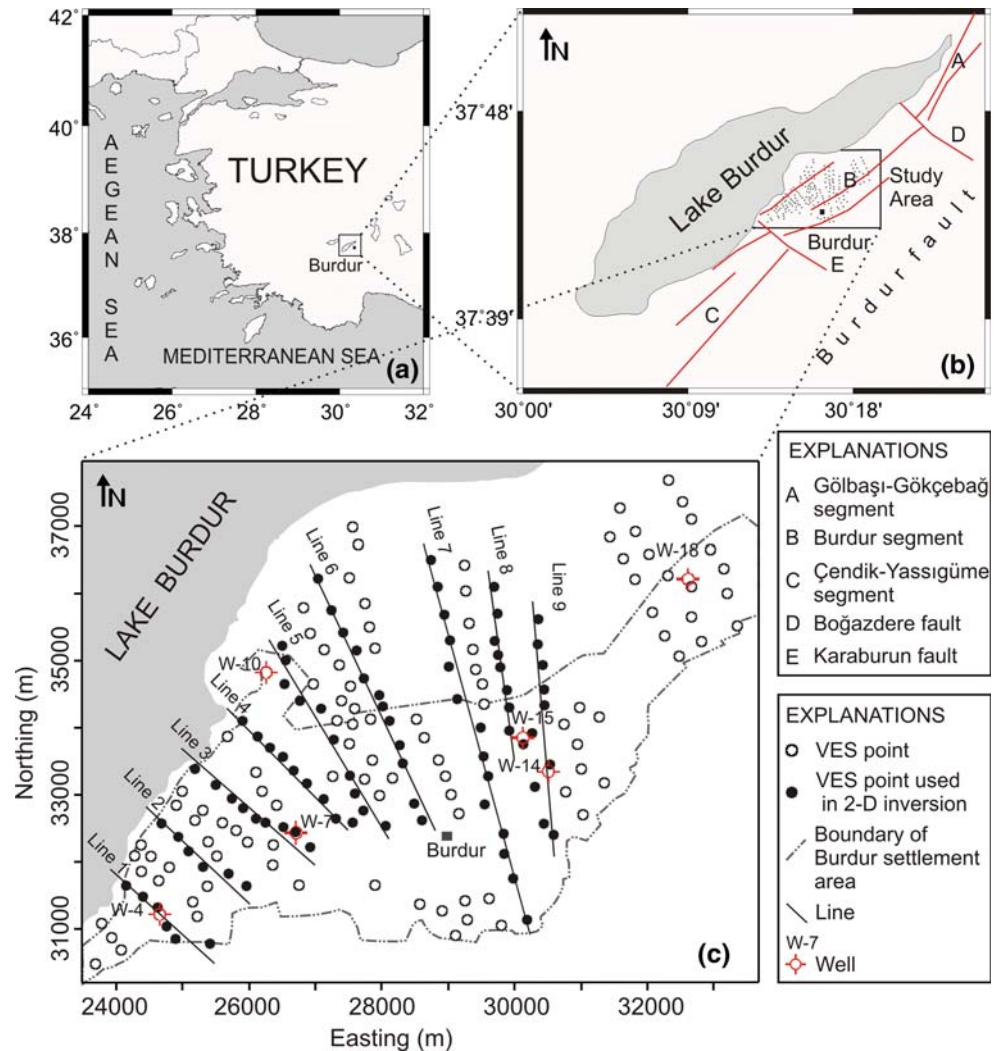
(2D) inversion techniques to obtain shallow geoelectrical structure, which might be used for determination of liquefaction potential in the study site. Also, using the results from 1D VES interpretation, we extended the groundwater level map, which was originally obtained by Davraz et al. (2003), toward north. Moreover, some of the VES data nearby the wells drilled during the project (Ertunç et al. 2001) were compared to the geological data from the wells (Fig. 1c). The present study indicates that the resistivity method provides useful results (e.g., water content of geologic units and determination of groundwater level) for the estimation of liquefaction potential in an area. Thus, we obtained a liquefaction hazard zonation map for the study area. The map was prepared by considering the resistivities resulted from 2D inversion of the VES profiles together with the groundwater level map and types of the sedimentary deposits observed in the field. The reason to use 2D interpretation was its ability to provide information on both vertical and horizontal extensions in the subsurface. In this paper, we discuss the results of the resistivity survey in

correlation with shallow geological structure and water content in the subsurface, which may control liquefaction potential in the study area. We also discuss the applicability of the resistivity data in determination of liquefaction-potential risk in a site by taking into account 2D interpretation of the VES-profiling data rather than 1D interpretation, which is a common approach to process VES data.

Tectonic and geologic setting

The study area is located in a region (SW Turkey), which is characterized by a number of normal faults and high seismicity (Bozkurt 2001; Verhaert et al. 2004). The main tectonic element is the Burdur fault (Fig. 1b). It is one of the most important active fault zones in the region yielding a number of earthquakes. The Burdur fault generated two large destructive earthquakes in October 1914 ($M_s = 7.0$) and May 1971 ($M_s = 6.2$) causing serious damage and

casualty (Ambraseys and Jackson 1998). It consists of three main segments in the direction of NE–SW (Fig. 1b), namely Gölbaşı-Gökçebağ, Burdur and Çendik-Yassıgüme (Ertunç et al. 2001). These segments are intersected by Boğazdere, Karaburun, Gölbaşı and Düger faults. Among them, the Gölbaşı and Düger faults are not shown on the map in Fig. 1b. The Burdur basin, which is a NE–SW trending half graben, is located at the eastern edge of the west Anatolian extensional province (Şengör et al. 1985; Price and Scott 1991).

A geologic map of the study area is shown in Fig. 2. The area consists of autochthonous alluvial cone, lacustrine alluvium and the Burdur formation including Yaka, Akdere and Gölcük Members (Gölcük not shown on the map) (Ertunç et al. 2001). In addition, allochthonous Gökçebağ Complex, which is out of the study area, has been displayed on the map.

The Quaternary lacustrine alluvium including clay, sand, silt and gravel extends along the Burdur Lake. Moreover, the Quaternary alluvial cone mainly consists of clay, gravel and sandy layers (Davraz et al. 2003). Both Şener et al. (2005) and Davraz et al. (2003) have described alluvium as a productive aquifer based on the existence of water within the sand and gravel beds. The Tertiary Burdur Formation including mainly pebble, sandstone, claystone, mudstone and marl is composed of three subunits as the Yaka, Gölcük and Akdere units (Davraz et al. 2003). The Yaka subunit has been generally described as travertine. Stream and lacustrine sediments constitute the Akdere subunit (Ertunç et al. 2001; Davraz et al. 2003). Figure 3 shows a generalized stratigraphical column in the study area.

Method and data acquisition

The VES measurements were taken at 189 points in the study site. This method is based on apparent resistivity measurements along the earth surface. An electric current is applied to the ground by means of two electrodes, and

Fig. 3 Generalized stratigraphical column in the study area (after Şener et al. 2005)

the potential difference is measured between two other electrodes. A VES equipment includes a resistivity meter, power source, two steel electrodes to inject the electric current into the ground, two nonpolarizable or steel electrodes for potential measurement, cables and reels for connection (Telford et al. 1990). The apparent resistivity value depends on the geometry of the current and the potential electrodes on the surface. Various electrode configurations, such as Wenner, Schlumberger, pole–pole, pole–dipole and dipole–dipole, are used in the field investigations. Among them, the Schlumberger array is commonly used in the VES studies (Fig. 4). In the present study, the data acquisition was performed using a Schlumberger array with a half-electrode spacing (AB/2) ranging from 1 to 100 m. In this configuration, the potential electrodes are put in a central position; the current ones are symmetrically placed in the outer sides. Then, the current electrodes are moved to the next
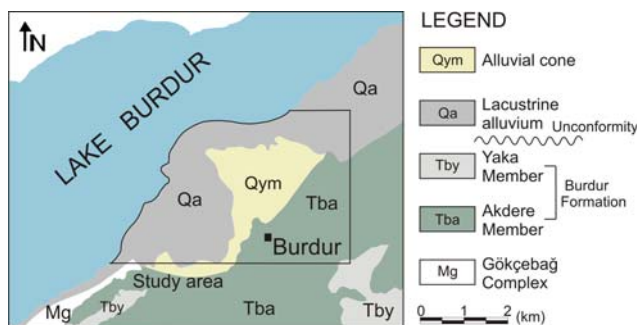

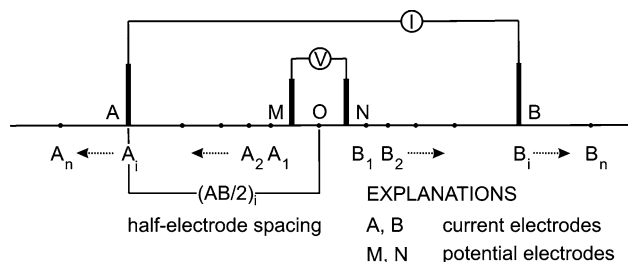**Fig. 2** Geological map of the study area (after Ertunç et al. 2001)

Fig. 4 Schematic Schlumberger electrode configuration for a VES survey

(AB/2)$_i$th position after each apparent resistivity measurement (Fig. 4). The depth of investigation can be increased by extending the distance between the current electrodes. On the other hand, the potential difference measured between the potential electrodes decreases due to the large distance between the current electrodes. In order to overcome this, the distance between potential electrodes should be increased to yield adequate potential (Telford et al. 1990; Binley and Kemna 2005; Ernstson and Kirsch 2006).

In order to interpret 1D VES data, IPI2win software has been used to generate a resistivity model best fitting between observed and calculated resistivities. This algorithm uses a linear filtering approach for the forward calculation of a wide class of geological models. The inverse solution is achieved by a regularized optimization (curve fitting) based on Tikhonov's approach (Bobachev et al. 2001).

The 2D interpretations were performed on 91 sounding locations showing an alignment along nine lines (Fig. 1c). The lines were mostly in the direction of NW–SE. Both the VES points and the extensions of the current electrodes were approximately along the lines. The inversion was performed using a code developed by Uchida and Murakami (1990). The code has a wide range of use from geothermal exploration (e.g., Ushijima et al. 2000; Özurlan et al. 2006) to archaeological prospection (e.g., El-Qady et al. 1999; Candansayar and Başokur 2001). It inverts apparent resistivity data from a sounding-profiling for 2D true resistivity distribution in the subsurface. This is achieved by using a linearized least-squares inversion with smoothness constraint based on a statistical criterion Akaike Bayesian Information Criterion (ABIC). In this scheme, subsurface is represented by a number of rectangular blocks, which have constant resistivity. The size of each block is kept constant during the inversion. Forward modeling for calculated resistivity data is carried out by finite-element method. The algorithm iteratively updates the resistivity of each block by minimizing the misfit between the observed and the calculated data (Uchida and Murakami 1990). A homogeneous model with a resistivity of an average of the observed data is generally used for the starting model. Based on the tests carried out by various starting models (10 times greater and 10 times smaller than the average value), Özurlan et al. (2006) reported that the algorithm yielded very similar results indicating the stability of the algorithm. In the present paper, we have tested the algorithm in the same way and reached the same conclusion. Therefore, we have used homogeneous initial models having the averages of the apparent resistivities measured along each line that 2D inversion was performed.

Results and discussion

Apparent resistivity maps

The apparent resistivity maps obtained for half-electrode spacings (AB/2) of 5, 10, 20, 50, 80 and 100 m are given in Fig. 5. According to the map, the study area displays almost similar features in the vertical direction with the increasing depth of investigation. Considering 25 Ωm contour line on each map, the study area may be divided into three main zones. These zones are called as A, B and C, and they are indicated on the map of 100 m. The zone B shows relatively higher resistivity values, whereas the zones A and C are generally characterized by low resistivity values. The zone A, located along the coastline of the Burdur Lake in the northwest of the study area, is dominated by low resistivity values (<25 Ωm). This low resistivity is explained by high water content in the sediments which is a result of intrusion from the lake. The zone B including mainly the metropolitan area of the city demonstrates apparent resistivities in the range of 25–200 Ωm. The resistivities gradually decrease with increasing half-electrode spacing, and it
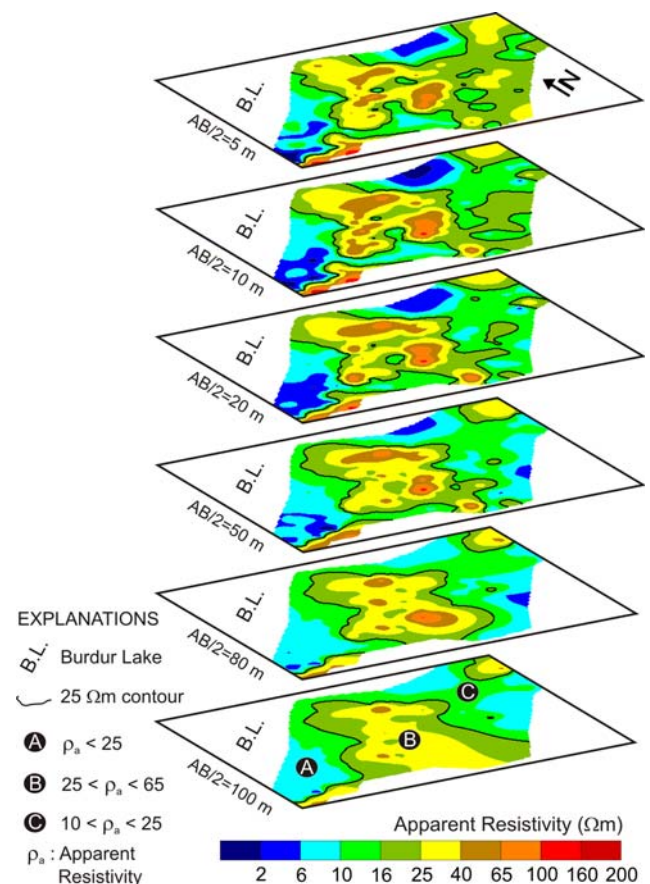

Fig. 5 Apparent resistivity maps for half-electrode spacings (AB/2) of 5, 10, 20, 50, 80 and 100 m, respectively

displays values changing from 25 to 65 Ωm at the (AB/2) spacing of 100 m. The zone C located in the northeastern part of the study area is not easily observed up to the (AB/2) spacing of 20 m. It is generally dominated by low resistivity values changing between 10 and 25 Ωm. Besides, the northeastern corner of each apparent resistivity map is distinguished by relatively high resistivities. Considering the geologic units in the study area, the low apparent resistivities are related with the Quaternary lacustrine alluvium and the Tertiary Akdere unit of the Burdur formation, and relatively high apparent resistivities are coincident with the Quaternary alluvial cone (see Fig. 2).

Comparison of VES and well data

Figure 6a–f shows the results of 1D interpretation of the data from the VES points of 7, 51, 77, 111, 121 and 177, respectively. RMS errors are in the range of 0.6–2.8%. In addition, Fig. 6g demonstrates a comparison among the results of the VES data and the wells, which are in the vicinity of each VES point. In Fig. 6g, the numbers on the column section on the left-hand side represent the resistivity values for the layers.

The VES-7 and the well W-4 are at the southwest of the study area and located on line 1. It is characterized by four low resistivity layers originating from the presence of groundwater and silty, clayey units. According to the well data, the depth to groundwater level is 20 m. The VES-51 in line 3 displays similar features to VES-7; it has higher resistivity values changing from 5 to 215 Ωm. The top high-resistive layer (162 Ωm) can be caused from dry soil on the surface. The second and third layers with the resistivities of 35 and 5 Ωm, respectively, correspond to silty and clayey units. The fourth layer with the highest resistivity (215 Ωm) is related to sandy material. The lowermost layer has a resistivity of 15 Ωm originating

Fig. 6 a–f Observed data, calculated curves and models obtained from 1D inversion of the VES points of 7, 51, 77, 111, 121 and 177, respectively. g Comparison of the models obtained from the VES data and the wells (well data after Ertunç et al. 2001)
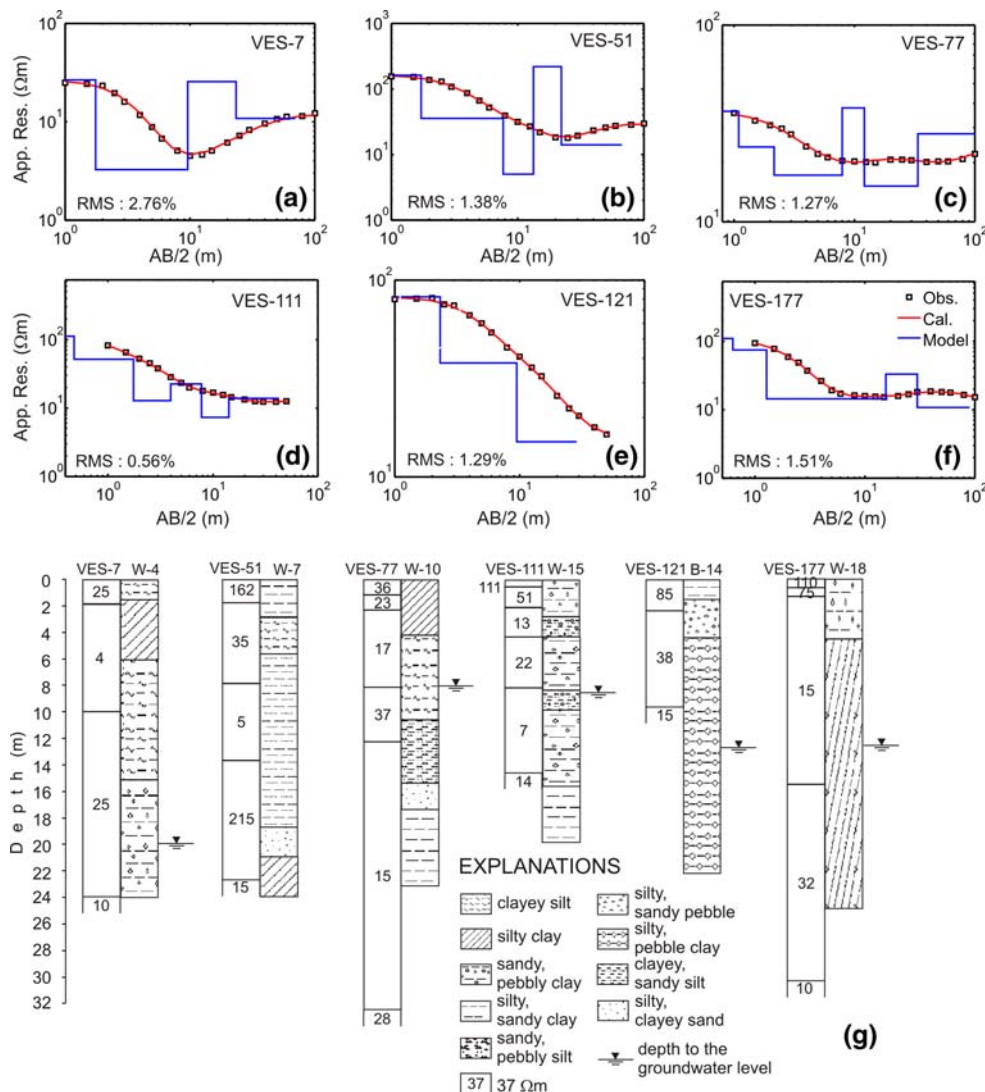
from clay content. Besides, there is no information regarding groundwater level in the W-7 data. This may indicate a deeper groundwater level, explaining higher resistivities at this location. The models at the VES points 77, 111, 121 and 177 are characterized by low resistivity values. This is in good agreement with the material observed in the wells near the VES locations. As seen from the well data, unconsolidated silty, clayey and sandy units are dominant in these wells. Also, shallow groundwater level around 10 m is a common feature in the wells. The effect of the groundwater on the resistivity curves is well observed, and this also explains low resistivities in the models. Generally, there is a good correlation between the models based on the resistivity method and the lithologies.

The groundwater level map

During the project, a groundwater level map (May 2000) was obtained for the study area using the data from a number of wells (Fig. 7a) and the groundwater flow direction was determined as being toward the Burdur Lake (Davraz et al. 2003). The map indicates a groundwater table elevation in the range of 860–960 m and it is around 860 m in the vicinity of the lake. As seen from Fig. 7a, the map does not provide enough information on the groundwater level in the northern part of the study area. On the other hand, there were a number of the VES points in this area, and the map was extended toward the north by determining the depth to the groundwater table from the resistivity sounding data. This was based on 1D interpretation of the VES data, and Fig. 7b displays this extended map. As shown from this figure, there is a very good agreement between the depths obtained from the wells and the resistivity measurements. The extended area is characterized by the groundwater table elevations ranging from 860 to 890 m. Regarding the effect of the groundwater on the soil liquefaction, determination of the depth to the water table by resistivity measurements on the surface is of great importance.

2D resistivity inversion

The results of the 2D resistivity inversion are displayed in Figs. 8 and 9. The RMS errors are generally less than 5% as indicated on each section, and they were obtained at the end of 5–8 iterations. All images display a depth range around 70 m. The data processing was performed along the nine lines with lengths ranging from 1,500 to 5,500 m. They are mostly in the direction of NW–SE. The VES points used in the inversion and the well locations on/near the lines are shown in each resistivity section. Topographical changes along the lines were also taken into
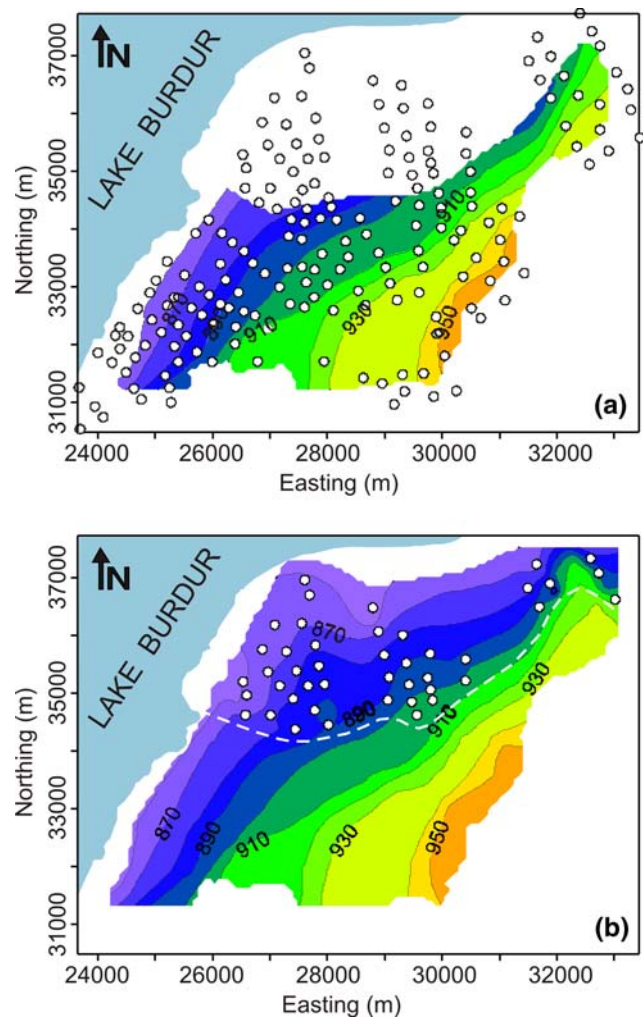

Fig. 7 a Map of the depth to the groundwater level (May 2000) (after Davraz et al. 2003) together with the VES points measured during the geoelectrical survey. b The same map extended toward north by the VES data. White dots show the VES points used in the extension of the map. White dashed line indicates the transition between the maps

account during the inversion. Each resistivity section provided results which are in good agreement with the geological units observed in the study area.

Lines 1–5 (Fig. 8a–e) traverse the Quaternary lacustrine sediments related with the Burdur Lake. Low-resistivity zones (3–25 Ωm) are the dominant features in the sections. Obviously, this low resistivity is the result of high water content of the sediments caused by the intrusions from the lake. High-resistivity zones (40–150 Ωm) are observed in the southeastern parts of the lines. This high resistivity might indicate the effect of the Quaternary alluvial cone deposits which overlie the lacustrine sediments in the vicinity of the southeastern ends of the lines (see Fig. 2). Most of the sections display lateral changes between low- and high-resistivity zones along the lines. But such a change is not a case on the line 2, whereas relatively high

resistivity in this section is observed as a top layer in the southeastern part of the line. Even though lines 3–5 display a gradual change between low and high resistivities, a sharp transition between resistivity zones is observed along line 1 in between the VES points 5 and 6. The high-resistivity zone is characterized by decreasing resistivity with respect to the depth, which reveals the effect of the groundwater. On the other hand, the sharp transition might be explained by the presence of a fault segment in the study area.

Lines 6–9 (Fig. 9a–d) traverse main geologic units in the study area. Lines 6 and 8 extend mostly over the Quaternary alluvial cone while lines 7 and 9 cut across the Tertiary Akdere member of the Burdur formation and the alluvial cone. These units are clearly identified on the sections by the resistivity values. The Quaternary alluvial cone is characterized by relatively high resistivities (40–150 Ωm). The Akdere unit, which includes stream and lacustrine sediments, is observed by very low-resistivity values (3–15 Ωm) indicating its high water saturation. This is particularly evident in the southeastern end of the line 7. Relatively low resistivity (14–28 Ωm) present in the northwestern ends of the lines 6, 7 and 8 are caused by the water-saturated lacustrine sediments. Similar to line 7, the southern part of the resistivity section along line 9

clearly illustrates the effect of the Akdere unit between the VES points 121 and 129. Overall, the sections display a decrease in resistivity with respect to the depth, revealing the existence of shallow groundwater level in the area.

Liquefaction hazard zonation map

We prepared a liquefaction hazard map for the study area (Fig. 10). This map was obtained by joint interpretation of the resistivity data, groundwater depth information from the extended groundwater level map and sediment types observed in the field since water saturation, type of deposits and depth to the groundwater level are the main parameters which control liquefaction phenomenon (e.g., Terzaghi et al. 1996). Table 2 shows the classification of the lique-faction potential risk based on the resistivity and sediment type. The resistivity ranges were determined according to the results of 2D inversion of the VES profiles. We defined three zones of liquefaction potential as very high, high and moderate for the study site.

According to Fig. 10, very high liquefaction-risk zone is observed along the shoreline of the Burdur Lake. This zone is characterized by very low resistivities ($3 < \rho < 15$ Ωm) indicating high water content in the subsurface, the Qua-ternary lacustrine and stream alluvium and shallow depth

Fig. 8 a–e Resistivity cross sections obtained from 2D inversion of the apparent resistivity data along the lines 1–5. Wells are also shown on the lines (f). Location map of the lines (Geologic units after Ertunç et al. 2001)
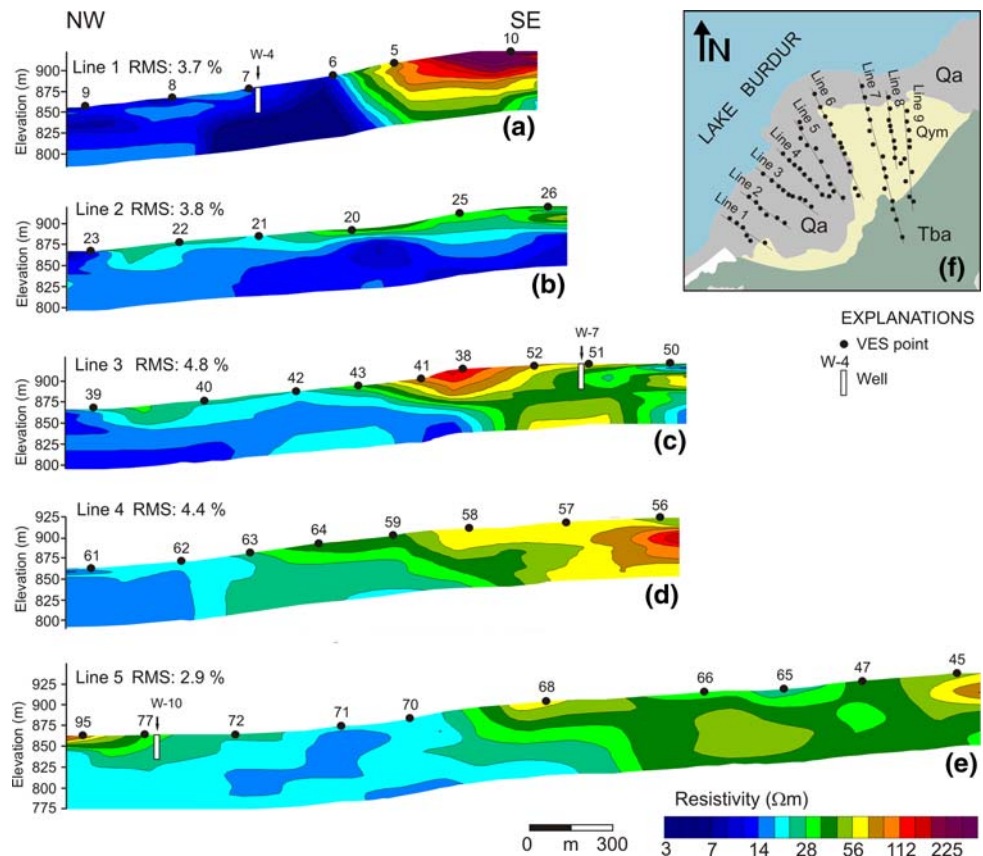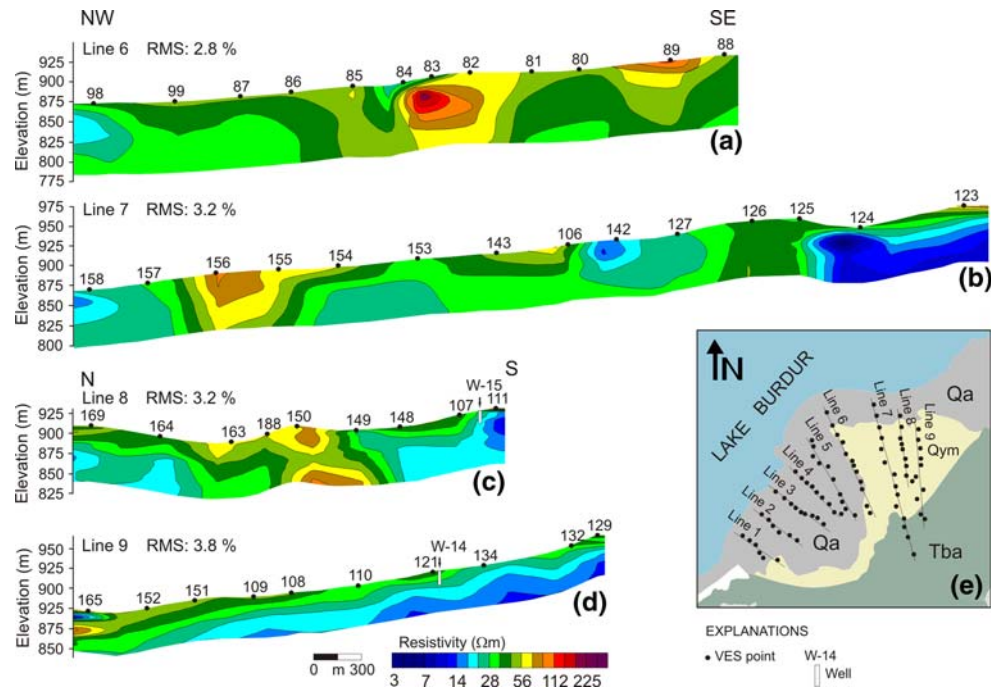
Fig. 9 a–d Resistivity cross sections obtained from 2D inversion of the apparent resistivity data along the lines 6–9. Wells are also shown on the lines (**e**). Location map of the lines (Geologic units after Ertunç et al. 2001)

to the groundwater level. The average depth is about 8 m in this zone. Two zones of high liquefaction risk are observed on the map. One zone is along the shoreline of the lake and the other is observed in the southeastern part of the study area. The zone along the shoreline is characterized by low resistivities ($15 < \rho < 30$ Ωm), the Quaternary alluvium and relatively higher average depth to the groundwater level, which is about 12 m. The other zone is represented by the Tertiary lacustrine and stream sediments, shallow

groundwater depth (about 9 m) and low resistivities ($15 < \rho < 30$ Ωm) (see Fig. 9). On the other hand, the zone of moderate liquefaction-potential risk is coincident with the Quaternary alluvial cone deposits. This zone has relatively higher resistivities ($30 < \rho < 150$ Ωm) and an average depth to the groundwater level about 12 m.

As seen from Fig. 10, the settlement area of the city is located in the southern part of the study area and the northern part is used for agricultural activities, thus mainly

Fig. 10 Liquefaction hazard zonation map for the study area. *Dots with the numbers* next to them indicate the VES points with the information of depth to the groundwater. Also the streams flowing across the study area are shown on the map (from Davraz et al. 2003). They are mainly dry streams except the rainy season
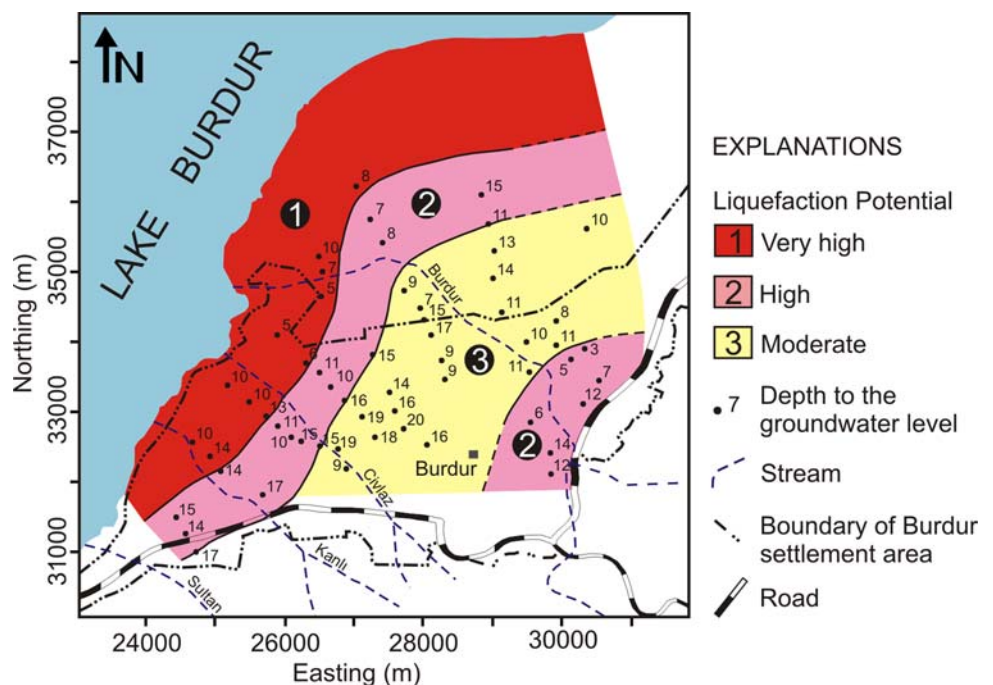
Table 2 Liquefaction potential based on resistivity inversion

Resistivity (Ωm)	Sediment type	Liquefaction potential
$3 < \rho < 15$	Lacustrine and stream	Very high
$15 < \rho < 30$	Lacustrine and stream	High
$30 < \rho < 150$	Alluvial cone deposits	Moderate

includes cultivated fields. Considering the location of the city's settlement area, the presence of the faults in the study area (see Fig. 1b) and the seismicity of the region, we may conclude that the city is under high liquefaction hazard risk.

Conclusion

In this paper, the results of a resistivity survey carried out in the city of Burdur, southwestern Turkey have been discussed. The data were processed by using both 1D and 2D inversion techniques to determine shallow resistivity structure, which could be used for the estimation of liquefaction risk in the study area. 2D interpretations were performed on a data set aligned along nine sounding profiles mostly trending in the direction of NW–SE. In general, the study area is characterized by the resistivities less than 150 Ωm, which are caused by the water-saturated and unconsolidated sediments (silty, clayey and sandy units) as observed in the wells. The lower resistivity is associated with both the Quaternary and the Tertiary lacustrine sediments while the relatively higher resistivity is related to the Quaternary alluvial cone deposits. The high water content is originated from shallow groundwater level as determined by both the resistivity and the hydrological studies performed in the survey site. As mentioned previously, geological conditions in the study site indicate soil liquefaction potential. The present study shows that the resistivity method of geophysics may provide useful information on vertical and horizontal extents of geologic units, water content in the subsurface and depth to the groundwater level, and this type of data might be useful for liquefaction studies. Thus, we prepared a liquefaction hazard map for the study area based on the results of this study. The resistivity data were interpreted together with the groundwater-depth information and types of the sedimentary deposits in the study site to classify liquefaction potential. In the present study, 2D interpretations of the VES-profiling data were used for liquefaction potential estimation rather than 1D interpretation of the resistivity data, which is a common approach in such studies. According to the map, the study area is characterized by high liquefaction hazard risk.

References

Ambraseys NN, Jackson JA (1998) Faulting associated with historical and recent earthquakes in the Eastern Mediterranean region. Geophys J Int 133:390–406

Balkaya Ç (2002) Burdur kentinin sığ yerelektrik yapısı. MSc, Suleyman Demirel University, Isparta, Turkey [in Turkish]

Beroya MAA, Aydin A (2007) First-level liquefaction hazard mapping of Laoag City, Northern Philippines. Nat Hazards 43:415–430

Binley A, Kemna A (2005) DC resistivity and induced polarization methods. In: Rubin Y, Hubbard SS (eds) Hydrogeophysics, Springer, Dordrecht, pp 129–156

Bird JF, Bommer JJ (2004) Earthquake losses due to ground failure. Eng Geol 75:147–179

Bobachev A, Modin I, Shevnin V (2001) IPI2WIN v.2.0, user's manual

Bozkurt E (2001) Neotectonics of Turkey—a synthesis. Geodin Acta 14:3–30

Candansayar ME, Başokur AT (2001) Detecting small-scale targets by the 2D inversion of two-sided three-electrode data: application to an archaeological survey. Geophys Prospect 49:13–25

Davraz A, Karagüzel R, Soyaslan II (2003) The importance of hydrogeological and hydrological investigations in the residential area: a case study in Burdur, Turkey. Environ Geol 44:852–861

Devi SP, Srinivasulu S, Raju KK (2001) Delineation of groundwater potential zones and electrical resistivity studies for groundwater exploration. Environ Geol 40:1252–1264

Edet AE, Okereke CS (2001) A regional study of saltwater intrusion in southeastern Nigeria based on the analysis of geoelectrical and hydrochemical data. Environ Geol 40:1278–1289

El-Qady G, Sakamoto C, Ushijima K (1999) 2-D inversion of VES data in Saqqara archaeological area, Egypt. Earth Planets Space 51:1091–1098

El-Qady G, Ushijima K, Ahmad ES (2000) Delineation of geothermal reservoir by 2D inversion of resistivity data at Hamam Faraun Area, Sinai, Egypt. Paper presented at the Proceedings World Geothermal Congress, Kyushu-Tohoku, Japan, May 28–June 10 2000, pp 1103–1108

Ernstson K, Kirsch R (2006) Geoelectrical methods. In: Kirsch R (ed) Groundwater geophysics a tool for hydrology. Springer, Heidelberg, pp 85–117

Ertunç A, Karagüzel R, Yağmurlu F, Türker A, Keskin N (2001) Report of the investigation of Burdur municipality and nearby surroundings in reference to earthquakes and residential communities (in Turkish). Suleyman Demirel University, Isparta

Frohlich RK, Urish DW, Fuller J, O'Reilly M (1994) Use of geoelectrical methods in groundwater pollution surveys in a coastal environment. J Appl Geophys 32:139–154

Gowd SS (2004) Electrical resistivity surveys to delineate groundwater potential aquifers in Peddavanka watershed, Anantapur District, Andhra Pradesh, India. Environ Geol 46:118–131

Hamzah U, Samsudin AR, Malim AP (2007) Groundwater investigation in Kuala Selangor using vertical electrical sounding (VES) surveys. Environ Geol 51:1349–1359

Hodlur GK, Dhakate R, Andrade R (2006) Correlation of vertical electrical sounding and boreholelog-data for delineation of saltwater and freshwater aquifers. Geophysics 71:G11–G20

Ibrahim EH, Elgamili MM, Hassaneen AGH, Soliman MN, Ismael AM (2002) Geoelectrical investigation beneath Behbiet ElHigara and ElKom ElAkhder archaeological sites, Samannud Area, Nile Delta, Egypt. Archaeol Prospect 9:105–113

Kanıbir A, Ulusay R, Aydan Ö (2006) Assessment of liquefaction and lateral spreading on the shore of Lake Sapanca during the Kocaeli (Turkey) earthquake. Eng Geol 83:307–331

Karlık G, Kaya MA (2001) Investigation of groundwater contamination using electric and electromagnetic methods at an open waste-disposal site: a case study from Isparta, Turkey. Environ Geol 40:725–731

Kundu N, Panigrahi MK, Sharma SP, Tripathy S (2002) Delineation of fluoride contaminated groundwater around a hot spring in Nayagarh, Orissa, India using geochemical and resistivity studies. Environ Geol 43:228–235

Lenkey L, Hámori Z, Mihálffy P (2005) Investigating the hydrogeology of a water-supply area using direct-current vertical electrical soundings. Geophysics 70:H11–H19

Majumdar RK, Majumdar N, Mukherjee AL (2000) Geoelectric investigations in Bakreswar geothermal area, West Bengal, India. J Appl Geophys 45:187–202

Özurlan G, Candansayar ME, Şahin MH (2006) Deep resistivity structure of the Dikili-Bergama region, west Anatolia, revealed by two-dimensional inversion of vertical electrical sounding data. Geophys Prospect 54:187–197

Park YH, Doh SJ, Yun ST (2007) Geoelectric resistivity sounding of riverside alluvial aquifer in an agricultural area at Buyeo, Geum River watershed, Korea: an application to groundwater contamination study. Environ Geol 53:849–859

Price SP, Scott B (1991) Pliocene Burdur basin, SW Turkey: tectonics, seismicity and sedimentation. J Geol Soc 148:345–354

Şener E, Davraz A, Özçelik M (2005) An integration of GIS and remote sensing in groundwater investigations: a case study in Burdur, Turkey. Hydrogeol J 13:826–834

Şengör AMC, Görür N, Şaroğlu F (1985) Strike–slip faulting and related basin formation in zones of tectonic escape: Turkey as a case study. In: Biddle KT, Christie-Blick N (eds) Strike–slip faulting and basin formation. Soc Econ Paleontol Mineral Sp Pub 37, pp 227–264

Song S, Lee J, Park N (2007) Use of vertical electrical soundings to delineate seawater intrusion in a coastal area of Byunsan, Korea. Environ Geol 52:1207–1219

Telford WM, Geldart LP, Sheriff RE (1990) Applied geophysics, 2nd edn. Cambridge University Press, Cambridge, p 770

Terzaghi K, Peck RB, Mesri G (1996) Soil mechanics in engineering practice, 2nd edn. Wiley, New York, p 549

Uchida T, Murakami Y (1990) Development of a Fortran code for the two-dimensional Schlumberger inversion. Geological Survey of Japan Open-File Report, No. 150, p 50

Ushijima K, Tagomori K, Pelton WH (2000) 2D inversion of VES and MT data in a geothermal area. Paper presented at the Proceedings World Geothermal Congress, Kyushu-Tohoku, Japan, May 28–June 10 2000, pp 1909–1914

US National Research Council (2003) Living on an Active Earth: perspectives on Earthquake Science. National Academy Press, Washington DC, p 418

Verhaert G, Muchez P, Sintubin M, Similox-Tohon D, Vandycke S, Keppens E, Hodge EJ, Richards DA (2004) Origin of palaeofluids in a normal fault setting in the Aegean region. Geofluids 4:300–314

Wessel P, Smith WHF (1995) New version of the generic mapping tools released. Eos 76:329

Wolf LW, Collier J, Tuttle M, Bodin P (1998) Geophysical reconnaissance of earthquake-induced liquefaction features in the New Madrid seismic zone. J Appl Geophys 39:121–129

Wolf LW, Tuttle MP, Browning S, Park S (2006) Geophysical surveys of earthquake-induced liquefaction deposits in the New Madrid seismic zone. Geophysics 71:B223–B230

Youd TL (1993) Liquefaction, ground failure and consequent damage during the 22 April 1991 Costa Rica earthquake. Abridged from EERI Proceedings: US Costa Rica Workshop. http://www.nisee.berkeley.edu/costarica/